scientific reports

Check for updates

OPEN

Thrombin induces degradation of murine intervertebral discs via angiogenesis and M1-like polarization of macrophages

Rikito Tatsuno[1], Takashi Ando[1,2]✉, Taro Fujimaki[1], Yoshihiro Takayama[3], Tetsuro Ohba[1] & Hirotaka Haro[1]

With the marked aging of the global population, the prevalence of musculoskeletal disorders due to low back pain has escalated, with an associated increase in the number of individuals requiring nursing care. To help identify novel therapies for treating disc degeneration, we examined the roles of thrombin and macrophages in intervertebral disc degeneration, a significant cause of low back pain. Experiments using a needle-puncture mouse tail model of disc degeneration confirmed that this process led to the production of thrombin and MCP-1. Thrombin altered macrophage markers, increasing the population of M1 markers and decreasing that of M2 markers. Therefore, increased thrombin and MCP-1 production may induce disc degeneration by inducing M1-type polarization of migrated macrophages. Disc tissue M1-macrophage levels were elevated 3 weeks after puncture. Administering SCH79797, a thrombin receptor (PAR1) antagonist, suppressed thrombin-induced disc degeneration and inhibited macrophage migration, M1 polarization, VEGF production, and angiogenesis. These findings suggest that the suppression of thrombin function in intervertebral disc inflammation is a novel and promising approach for treating disc degeneration.

Keywords Disc degeneration, Low back pain, Thrombin, Macrophage polarization, Angiogenesis

Low back pain affects all generations, from adolescents to the elderly; further, low back pain, especially in the elderly, is associated with frailty and sarcopenia, which interfere with exercise and well-being[1]. This global health issue affected 619 million people in 2020 and is projected to increase to 843 million by 2050, owing to population growth and aging[2,3]. Low back pain reduces quality of life, prevents people from working, and imposes a significant economic burden[4–7]. "Non-specific" low back pain refers to pain not explained by other diagnoses, such as underlying disease, pathology, or tissue damage [8]. Risk factors include low physical activity, smoking, obesity, and high physical stress at work [9].

Physiological intervertebral discs lack blood vessels and consist primarily of a cartilage matrix. Inflammation and sensory nerve intrusion due to disc degeneration cause low back pain [10–14]. Vascular invasion of the outer annulus fibrosis has been observed in degenerated discs, but the inflammatory process in disc degeneration remains unclear [15–17].

We previously employed magnetic resonance imaging (MRI) and reported spontaneous regression of herniated discs, with contrast-enhanced MRI revealing more cases of regression [18,19]. Examination of surgically excised herniated discs revealed inflammatory cell infiltration, primarily by macrophages. Stimulation of mouse intervertebral discs with inflammatory cytokines increased vascular endothelial growth factor (VEGF) production and promoted angiogenesis in the discs [20].

Thrombin (coagulation factor IIa), produced from prothrombin by factor Xa, plays a central role in blood coagulation and is closely associated with inflammatory and immune responses [21,22]. In cultured murine intervertebral discs, thrombin administration induces matrix metalloproteinase 3 (MMP3) production and disc degeneration [23]. In human primary nucleus pulposus culture, thrombin induces epidermal growth factor receptor expression and disc degeneration [24].

[1]Department of Orthopedic Surgery, Faculty of Medicine, University of Yamanashi, 1110 Shimokato, Chuo, Yamanashi 409-3898, Japan. [2]Department of Rehabilitation, Koshu Rehabilitation Hospital, Yamanashi, Japan. [3]Department of Orthopedic Surgery, Yamanashi Kosei Hospital, Yamanashi, Japan. ✉email: tando@mtg.biglobe.ne.jp; tttando0817@gmail.com

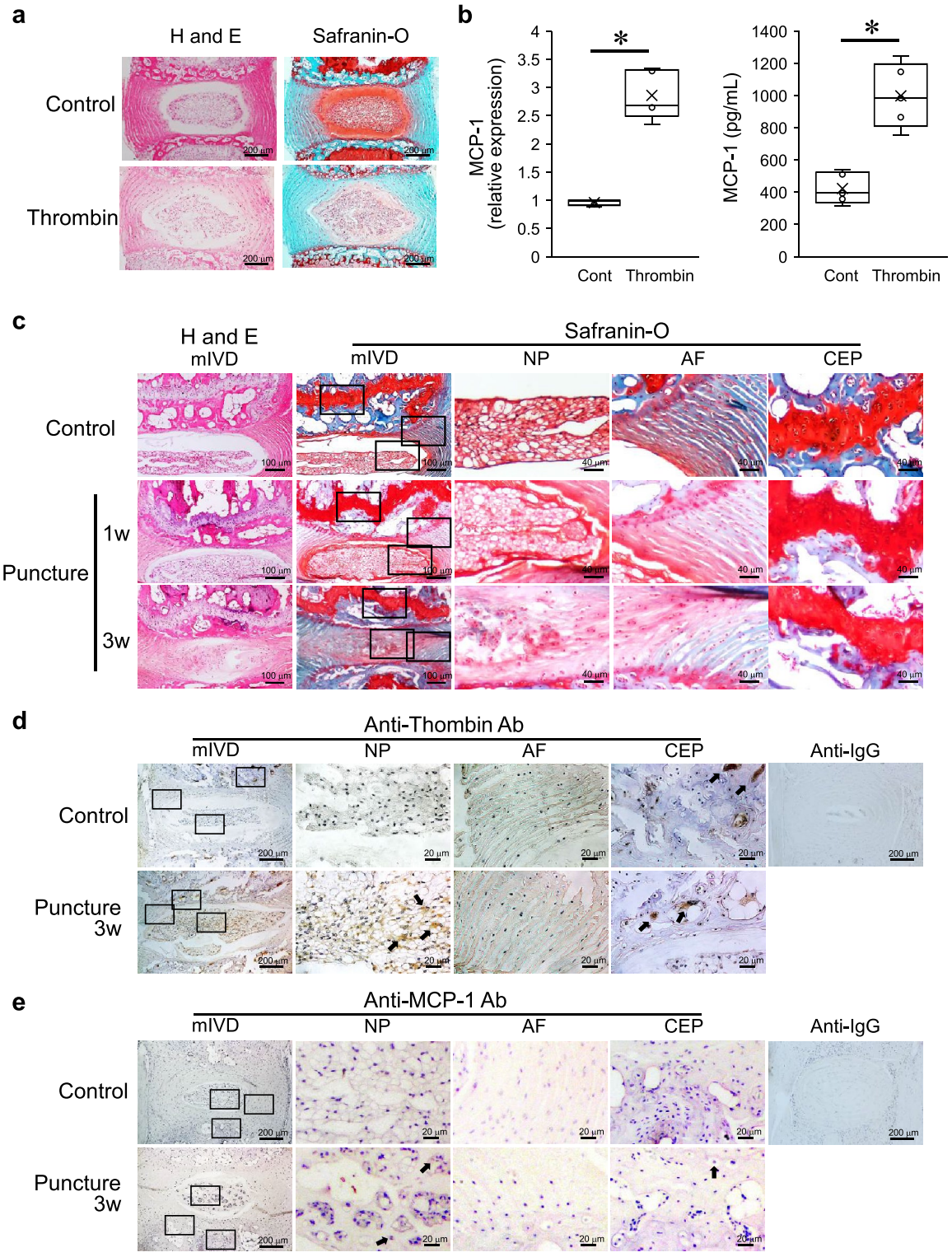

The balance between M1 and M2 macrophage populations is critical in immune responses. Of the two macrophage subtypes, M1 macrophages are induced during tissue damage and inflammation, whereas M2 macrophages act in tissue repair [25,26]. Several markers indicating macrophage polarization have been identified [27]. Previous reports have used iNOS and CD86 as M1 markers, CD163 and arginase-1 as M2 markers, and Iba1 as a general macrophage marker. In intervertebral disc degeneration, M1 macrophages initially dominate, switching to M2 dominance over time [28], with differences in polarization depending on the degree of degeneration [29,30]. However, the roles of M1 and M2 macrophage infiltration and polarization in intervertebral disc inflammation remain unclear.

Therefore, we hypothesized that thrombin induces macrophage polarization and promotes degeneration in mouse intervertebral discs. Clarifying these mechanisms may help establish novel therapies for intervertebral disc degeneration.

◀**Fig. 1**. Comparison of ex vivo (mouse intervertebral disc [mIVD] organ-culture system) and in vivo (puncture model) intervertebral disc degeneration. (**a**) H&E and Safranin-O staining of mIVDs cultured in an organ culture system in the presence or absence of 100 nM thrombin for 72 h. (**b**) mIVDs were stimulated with thrombin, and quantitative PCR was performed using specific primers for *Mcp1* ($p = 0.043$). Significance was determined using the Mann–Whitney U-test (left panel). Culture supernatants were collected to measure the MCP-1 concentration via ELISA ($p < 0.001$). Significance was determined using Student's t-test (right panel). (**c**) H&E and Safranin-O staining of the punctured mIVDs in the in vivo puncture model. (**d, e**) Immunohistological analysis of thrombin and MCP-1 (brown staining) expression in the nucleus pulposus (NP), annulus fibrosis (AF), and cartilage endplate (CEP) [right] at high magnification and in whole mIVDs (left) at low magnification. Images using an IgG isotype control antibody are included to demonstrate the specificity of the IHC staining. Three mice were used in each experiment, from which eight to nine intervertebral discs per mouse were collected. Values represent the mean ± SD. *$p < 0.05$, relative to the corresponding control.

Results

Ex vivo and in vivo disc degeneration induces thrombin and monocyte chemotactic protein-1 (MCP-1)

To elucidate the mechanisms of disc inflammation, we compared an ex vivo model with an in vivo puncture model. Murine intervertebral discs (mIVD) were cultured in an organ culture system in the presence or absence of 100 nM thrombin for 72 h. Under unstimulated conditions, Safranin-O dye specifically binds to acidic proteoglycans present in the cartilage matrix, forming a reddish-orange complex around the nucleus pulposus and cartilage endplate cells. In the presence of thrombin, mIVD degradation was confirmed by the loss of Safranin-O staining after 72 h of culture (Fig. 1a). Thrombin stimulation increased monocyte chemotactic protein-1 (MCP-1) expression, as confirmed using quantitative real-time PCR ($p = 0.043$) and ELISA ($p < 0.001$) (Fig. 1b).

In vivo, in the tail puncture model, punctured mIVDs exhibited reduced Safranin-O staining, with morphological degeneration over time (Fig. 1c). Immunostaining revealed a tendency for thrombin and MCP-1 expression to be elevated in punctured mIVDs, especially in the nucleus pulposus and cartilage endplate (Fig. 1d, e). Disc degeneration and thrombin and MCP-1 production were therefore observed both ex vivo and in vivo.

Thrombin tends to induce M1 macrophage polarization

Next, we examined the effects of thrombin on MCP-1-induced macrophages. PCR revealed that thrombin stimulation of mouse bone marrow macrophages increased the levels of CD86, a common M1 marker, and reduced those of CD163, an M2 marker (Fig. 2a). Western blotting revealed that thrombin stimulation increased the expression of both M1 markers, CD86 and iNOS, and reduced that of M2 markers, CD163 and arginase (Fig. 2b; Supplementary Fig. S1). These results indicate that thrombin tended to induce M1-type polarization.

In vivo mouse tail puncture induces M1 macrophages

We confirmed macrophage polarization in vivo by examining mIVDs in the tail puncture model. At 3 weeks after treatment, mIVDs were collected for immunostaining and purified, and protein levels were quantified. Based on immunostaining, the expression of Iba1, a macrophage marker, was higher in the punctured discs than it was in the control discs. Staining for the M1 marker iNOS was stronger in the punctured mIVDs than it was in the control, whereas staining for the M2 marker arginase was negligible in both punctured and control mIVDs (Fig. 3a). The tail puncture model exhibited significantly higher CD86 expression ($p = 0.0040$) and lower CD163 expression ($p = 0.0013$) than those of the control, based on western blotting and immunostaining (Fig. 3b, c; Supplementary Fig. S2, S3). These findings suggest that macrophages infiltrating the puncture mIVDs of the tail in vivo were predominantly M1 macrophages.

PAR1 antagonist SCH79797 suppresses thrombin-induced mIVD degeneration

We hypothesized that, in the puncture model of the mouse tail, thrombin induces M1-type macrophages, causing disc degeneration. We therefore examined whether this degeneration could be suppressed by inhibiting proteinase-activated receptor 1 (PAR1), the major receptor for thrombin. In the punctured model, safranin staining of chondrocytes in the nucleus pulposus and endplates declined significantly over time ($p = 0.02$), whereas this did not occur in the healthy control (Fig. 4a; Supplementary Fig. S3). A disc degeneration score was generated [31]. At 3 weeks after puncture, the group treated with SCH79797, a PAR1 antagonist, showed significantly less disc degeneration than that of the vehicle group (Fig. 4b; Supplementary Fig. S4).

PAR1 antagonist inhibits thrombin production and macrophage M1 polarization

Thrombin production and macrophage polarization were examined to elucidate the mechanisms by which the PAR1 antagonist suppresses disc degeneration. At 3 weeks after tail puncture, the mIVDs were removed and immunostained. Thrombin expression was higher in punctured discs than it was in the controls, but was inhibited by the PAR1 antagonist. The level of CD86 was slightly elevated in the punctured discs, which was abrogated by the administration of the PAR1 antagonist. iNOS was elevated in the control discs and was further increased by the puncture discs. This increase in iNOS due to the puncture was reduced by the administration of the PAR1 antagonist. On the other hand, CD163 expression was low in control mIVDs and showed little change after puncture or administration of a thrombin antagonist (Fig. 5).

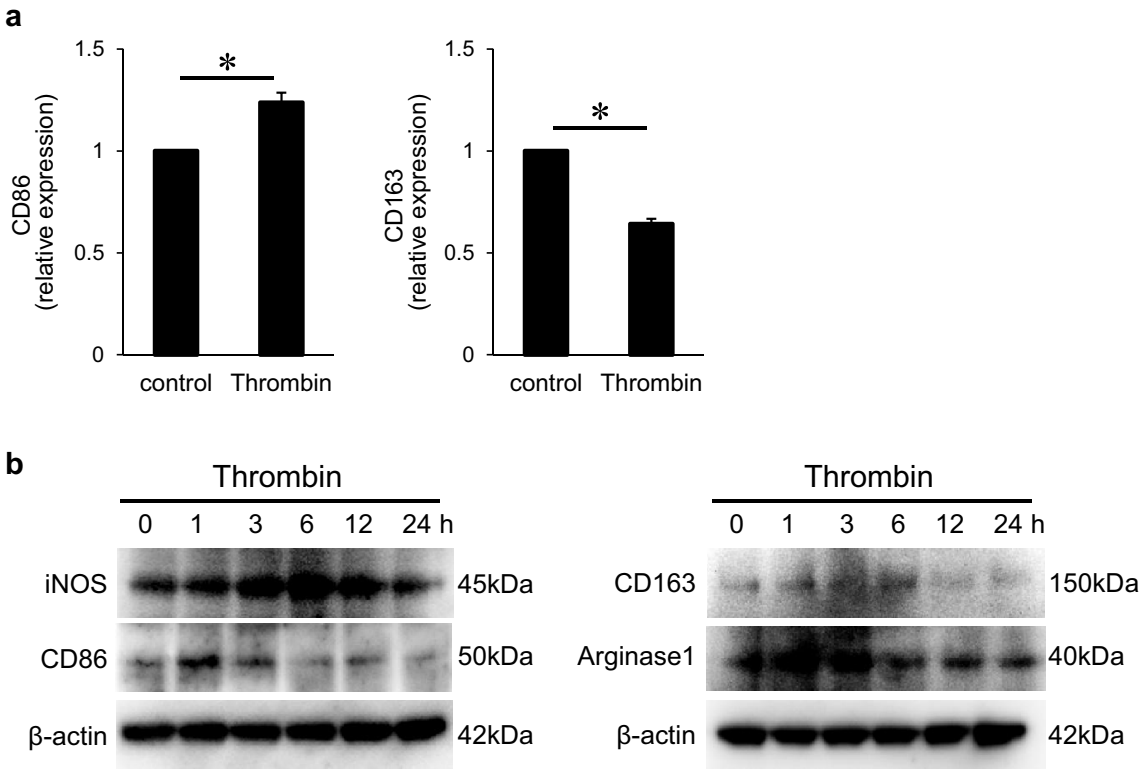

Fig. 2. Thrombin promotes polarization into M1 macrophages. (**a**) Mouse bone marrow was stimulated with thrombin, and quantitative PCR was performed using specific primers for *CD86* and *CD163*. Biological and technical replicates were performed three times. (**b**) Mouse bone marrow was stimulated with thrombin, and western blotting was performed using antibodies for the M1 markers iNOS and CD86, and the M2 markers CD163 and Arginase-1. β-actin was used as an internal control. n = 3. Values represent the mean ± SD. $^{*}p < 0.05$, $^{**}p < 0.01$, relative to the corresponding control.

Thrombin induces VEGF production and angiogenesis

Finally, VEGF production and angiogenesis, which are important factors in disc degeneration, were investigated in the ex vivo and in vivo tail puncture models. Ex vivo, mIVD cells from the control and thrombin-treated groups, with or without PAR1-antagonist treatment, were incubated in a disc culture system for 72 h to generate intervertebral disc RNA, and the supernatant was collected. qPCR analysis revealed that thrombin increased the levels of VEGF RNA in the mIVD, whereas inhibition of PAR1 suppressed this (Fig. 6a, left panel). Quantification of VEGF in the culture supernatant using ELISA generated similar results (Fig. 6a, right panel).

At 3 weeks after puncture treatment, the mIVDs were removed and immunostained. VEGF expression was higher in punctured discs than that in the healthy controls, but this increase was abrogated by PAR1-antagonist administration. Relative to the controls, the punctured discs exhibited stronger staining for VEGF and CD31, a platelet-endothelial cell-adhesion molecule, around the nucleus pulposus, whereas this was abrogated by the PAR1 antagonist (Fig. 6b, Supplementary Fig. S5).

Discussion

Intervertebral disc degeneration involves multiple processes, including changes in gene expression, stress responses, cellular senescence, and blood supply-related nutritional status. To further elucidate these processes, we examined the roles of thrombin and macrophage polarization in the pathogenesis of intervertebral disc degeneration. In vivo, we confirmed thrombin and MCP-1 production in the puncture model, consistent with our prior ex vivo findings [23,32]. The puncture model exhibited a higher proportion of M1-type macrophages and VEGF and CD31 production than those of the healthy control. Administration of SCH79797, a PAR1 antagonist, reduced disc degeneration by suppressing these processes. These results suggest that thrombin causes inflammatory M1-type macrophage polarization during disc degeneration and that PAR1 antagonists may be potential therapeutic candidates.

Needle puncture, a common method for inducing intervertebral disc degeneration, was used to examine both thrombin expression in the injured discs and the effects of thrombin on macrophages. These findings reveal that thrombin acts on the intervertebral disc, inducing the expression of MCP-1 (a chemotactic factor for macrophages), VEGF, and angiogenesis; this suggests that thrombin creates an environment supporting macrophage infiltration into the disc tissue. In the presence of thrombin, M1 macrophage marker expression was significantly elevated, and these markers were strongly expressed in the puncture model. M1 macrophages, which exert bactericidal effects by producing proinflammatory cytokines, are induced by IFN-γ, lipopolysaccharides

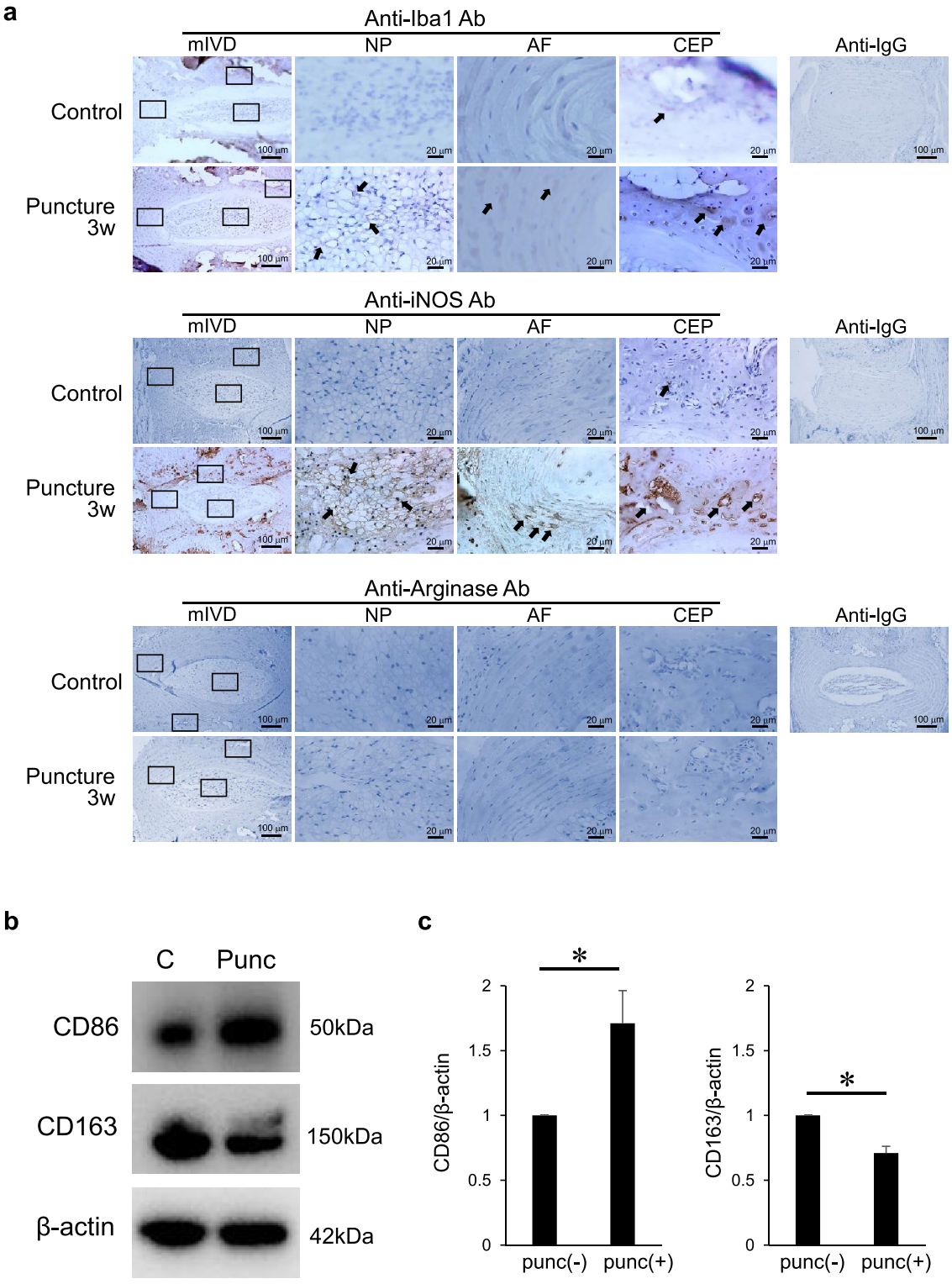

Fig. 3. M1 macrophages were induced in the in vivo mouse intervertebral disc (mIVD) degeneration model (puncture model). (**a**) Immunohistological analysis of Iba-1, iNOS, and arginase (brown staining) expression in nucleus pulposus (NP), annulus fibrosis (AF), and cartilage endplate (CEP) [right] at high magnification and in whole mIVDs (left) at low magnification. Images using an IgG isotype control antibody are included to demonstrate the specificity of the IHC staining. (**b**) Protein was extracted from punctured mIVDs in the puncture model, and western blotting was performed using antibodies against CD86, CD163, and β-actin. (**c**) Images of the panel in (**b**), captured using a ChemiDoc Touch system and quantified using ImageJ. Biological and technical replicates were performed three times. Values represent the mean ± SD. $^{*}p < 0.05$, $^{**}p < 0.01$, relative to the corresponding control.

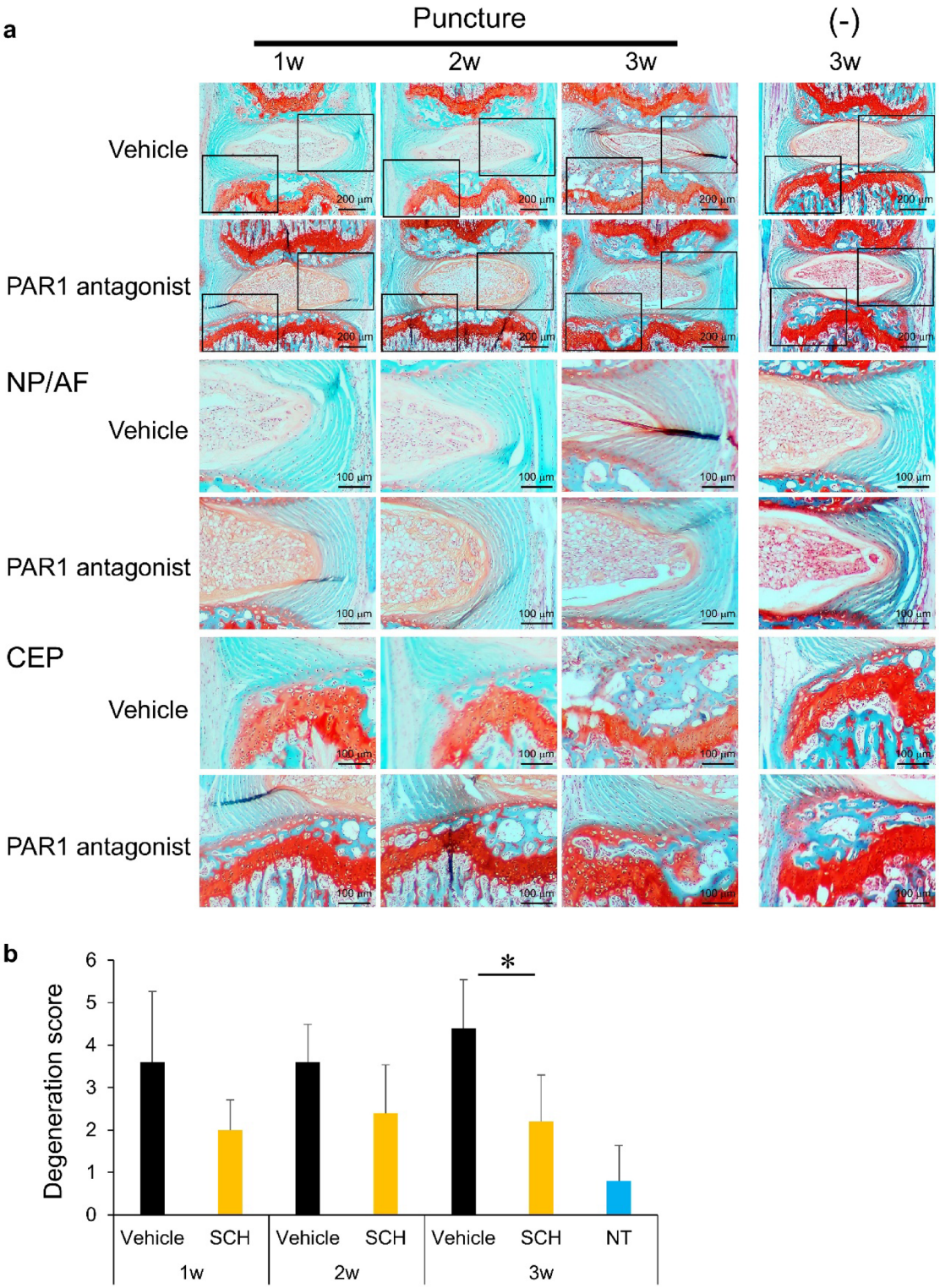

Fig. 4. Thrombin induces mouse intervertebral disc (mIVD) degeneration via the action of the thrombin receptor PAR1. (**a**) In the puncture model, intervertebral disc tissue was obtained at weeks 1, 2, and 3 weeks after puncture, with or without PAR1-antagonist treatment; samples were stained with Safranin-O and fast green. (**b**) Quantification of the findings in panel (**a**) using a degeneration score. Three mice were used in each group. Values represent the mean ± SD. *$p < 0.05$, relative to the corresponding control.

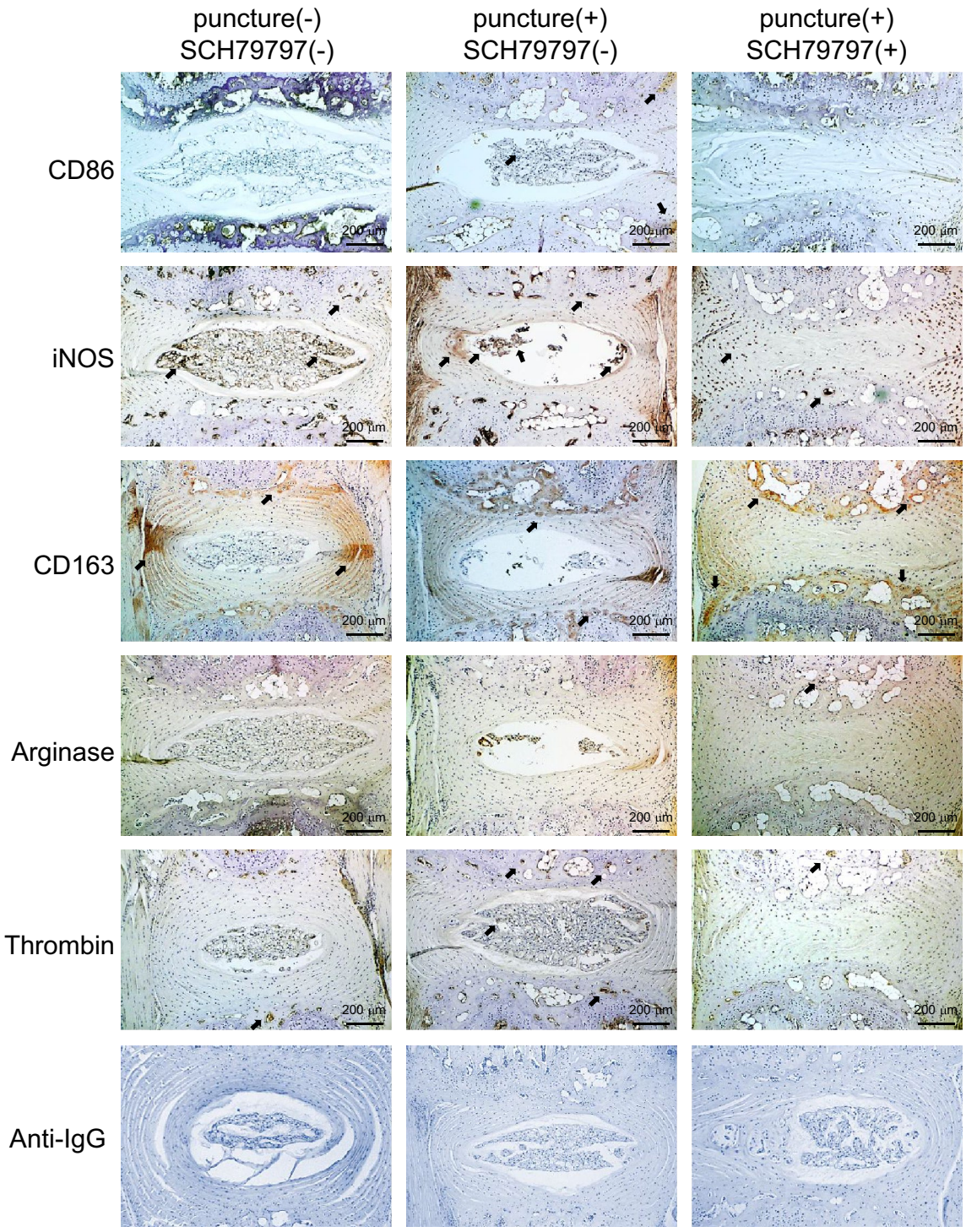

Fig. 5. PAR1 antagonist abrogates macrophage M1 polarization and angiogenesis. Intervertebral disc tissue was obtained from the puncture model 3 weeks after puncture, with or without PAR1-antagonist treatment. Immunostaining was performed using antibodies against CD86, iNOS, CD163, arginase, and thrombin. Images using an IgG isotype control antibody are included to demonstrate the specificity of the IHC staining. Three mice were used in each group.

LPS, or TNF-α, and exhibit overexpression of CD80, CD86, and iNOS [33]. In contrast, M2 macrophages, which play important roles in tissue repair, angiogenesis, and metabolism, are induced by anti-inflammatory factors such as IL-4, IL-10, IL-13, TGF-β, and glucocorticoids, and exhibit overexpression of Arg-1, CD163, and CD206 [34,35]. Here, we examined the polarization of thrombin-polarizing naive macrophages to the M1 type; while such findings are valuable in many fields, these have been rarely reported in the context of thrombin mediated disc degeneration [36].

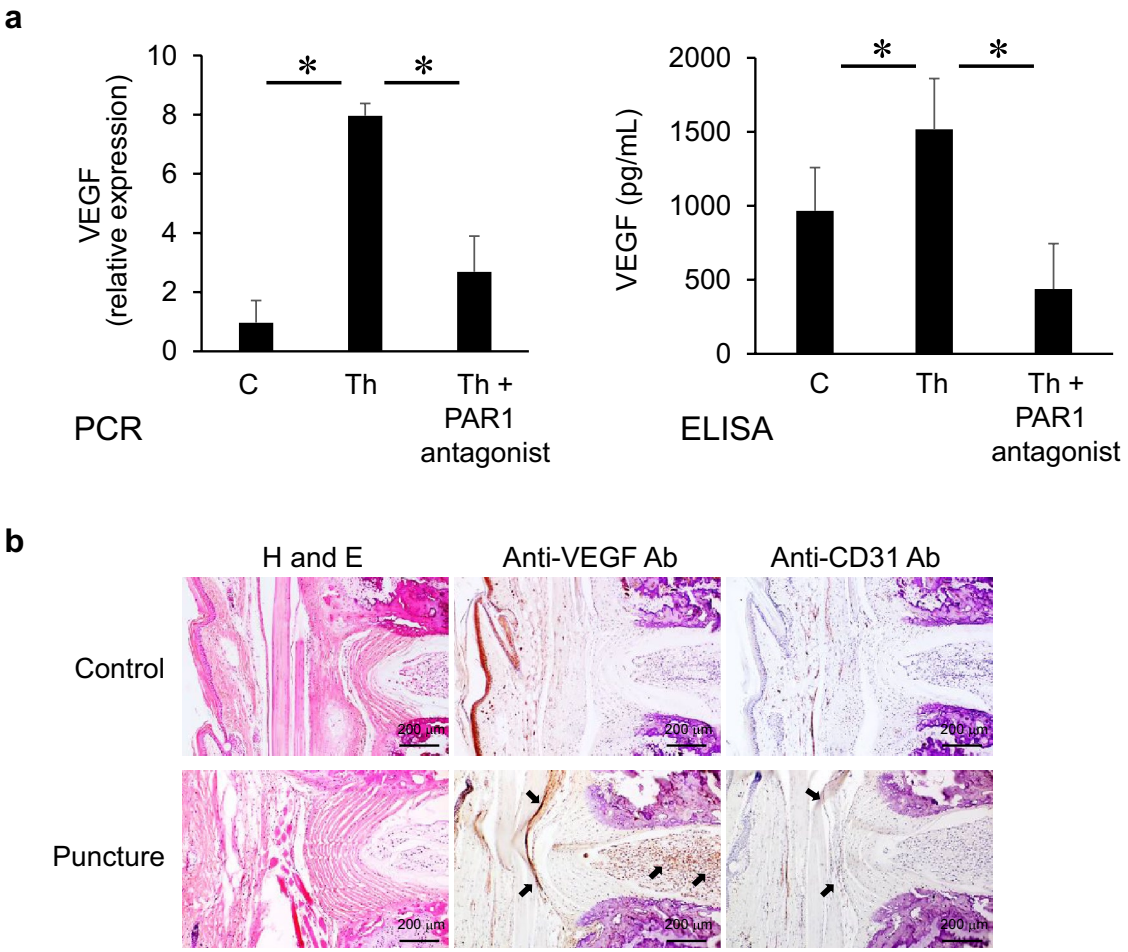

Fig. 6. Thrombin induces VEGF production and angiogenesis. (**a**) Mouse intervertebral discs (mIVDs) were stimulated with thrombin with or without PAR1-antagonist treatment, and quantitative PCR was performed using specific primers for *VEGF*. The culture supernatant was collected to measure the VEGF concentration via ELISA. (**b**) Intervertebral disc tissue was obtained 3 weeks after puncture and from healthy controls. Immunostaining was performed using antibodies for VEGF and CD31. Three mice were used in each group. Values represent the mean ± SD. $^{*}p < 0.05$ or $^{**}p < 0.01$, relative to the corresponding control.

The puncture model exhibited the production of thrombin and MCP-1, disc degeneration, macrophage migration to the degenerated disc, and abundant M1 macrophage production. To clarify whether these events were inflammatory mechanisms caused by thrombin or were independent events, we tested the effects of SCH79797, a PAR1 antagonist, in the puncture model. SCH79797 administration abrogated the enhanced disc degeneration, M1 macrophage polarization, and the migration of both M1 and M2 types. This suggests that, following disc puncture, thrombin production causes inflammation, leading to polarization, causing disc degeneration.

PAR1 participates centrally in thrombin-induced platelet aggregation. In a prior study, PAR1-knockout mice did not exhibit spontaneous bleeding; a PAR1-antagonist was established as an antiplatelet agent to reduce bleeding [37–39]. This PAR1-antagonist, approved by the FDA in 2014 as vorapaxar and in clinical use for 10 years, reduces the risk of heart attack, stroke, and death due to cardiovascular events [40]. It is administered orally, making it relatively safe and easy to take [41]. The incidence of disc degeneration, myocardial infarction, stroke, and cardiovascular death is very high in individuals older than 50 years of age [42]. Considering that the age range of clinical morbidity for these vorapaxar-indicated conditions is close to that of patients with lumbar disc degeneration, vorapaxar administration may effectively treat degenerative disc disease, possibly caused by chronic inflammation, in patients with back pain that has persisted for over 3 months without responding to standard analgesic medications.

This study had some limitations. First, when selecting animal models, it is important to choose those whose mechanisms of intervertebral disc degeneration are similar to those in humans; the models must also be able to generate consistent and reproducible outcomes and must be cost-effective and easy to maintain. However, the fact that mice are quadrupedal makes it difficult to subject their intervertebral discs to the same gravitational loading as those of bipedal humans. Therefore, a tail puncture model was used to artificially induce disc degeneration. Second, our findings suggest that thrombin stimulation induces an M1-type polarization

tendency in macrophages. Nonetheless, it is possible that the puncture injury directly induced M1 macrophage production. Third, while we found that thrombin and M1 macrophages were induced in mIVDs in the tail puncture model, and that disc degeneration occurred, we did not examine whether the induced macrophages were directly responsible for disc degeneration. Fourth, there is a possibility that bone marrow may have been inadvertently included during the isolation of mouse coccygeal intervertebral discs. The presence of bone marrow could lead to staining of resident macrophages in IHC and may also influence macrophage polarization. To minimize this risk, all intervertebral discs were dissected under a microscope, and a new scalpel blade was used for each procedure without exception. Finally, only male mice were used in this study; if female mice were used, the experimental results may be different.

Using an in vivo tail puncture model experimental system, we found that thrombin plays a vital role as a proinflammatory cytokine in causing intervertebral disc degeneration, consistent with our prior ex vivo model findings [23,32,43,44]. The thrombin produced in mouse intervertebral discs may promote angiogenesis and migration of macrophages, which then polarize into the inflammatory M1 type. Finally, inhibition of the thrombin receptor PAR1 by a PAR1 antagonist abrogated macrophage polarization to the M1 type and suppressed intervertebral disc degeneration. Future research should focus on translating these findings into clinical trials to evaluate the efficacy and safety of PAR1 antagonists in humans. Additionally, further investigation is needed to elucidate the detailed molecular mechanisms underlying thrombin-induced inflammation and macrophage polarization in disc tissues. Finally, these findings may potentially help improve outcomes for patients with low back pain and enhance the quality of life for patients with degenerative disc diseases.

Materials and methods

Animals

All methods were carried out in accordance with relevant guidelines and regulations. All methods are reported in accordance with the ARRIVE guidelines (https://arriveguidelines.org), 2020 AVMA guidelines (https://www.avma.org), and Proper Conduct of Animal Experiments of the Science Council of Japan guidelines (https://www.scj.go.jp/en/animal). The protocols were approved by the Animal Care and Use Committee of the University of Yamanashi (No. A28_38).

Homozygous WT C57BL/6 J male mice (5–6 weeks old) were purchased from CLEA Japan, Inc. (Tokyo, Japan). The mice were housed at 22–24 °C under a 12 h light/dark cycle and were fed standard mouse chow. Water was provided ad libitum. Mice were divided into a tail puncture group and control group (without treatment). In the tail puncture group, eight to nine coccygeal intervertebral discs were punctured under anesthesia using a 27-gauge needle (Supplementary Fig. S6). There were three mice in each group. This method is less invasive and time-consuming than are other methods, and allows precise control of the extent and location of injury [45,46]. We administered SCH79797 at a concentration of 10 mM via intravenous injection twice a week for 3 weeks. All mice were euthanized for histological analysis 1, 2, or 3 weeks after treatment. Anesthesia was performed using the XGI-8 Veterinary Gas Anesthesia System (PerkinElmer, MA, USA). A vaporizer provided the appropriate concentration of isoflurane, and the concentration was introduced at 4–5% and maintained at approximately 2–3%. Euthanasia was performed using a non-prefilled chamber infused with CO_2 from a commercially available cylinder with a fixed pressure regulator and in-line restrictor, with gas flow controlled to 30–70% of the chamber volume per minute, conforming to the ARRIVE 2.0 and 2020 AVMA guidelines [47].

Murine intervertebral disc organ culture

The coccygeal murine intervertebral disc (mIVD) organ-culture system was prepared as previously described [32]. Briefly, mIVD tissue specimens were obtained from the tail bones of mice using a dissecting microscope after the skin and soft tissues were removed. To avoid contamination with bone marrow, tissue samples were collected under a microscope, and a new scalpel was used for each procedure. Whole mIVD tissue specimens were cultured at 37 °C in 12-well plates in 1 mL of Dulbecco's modified Eagle's medium (DMEM; Invitrogen/Gibco; Thermo Fisher Scientific, MA, USA) containing 0.1% FBS with or without thrombin (100 nM) obtained from Prolytix (Essex Junction, VT, USA), or with or without SCH79797 (a PAR1 antagonist; Santa Cruz Biotechnology, Inc.; TX, USA).

Tissue histological analysis

Histological analysis was performed as previously described [48]. The mIVDs were fixed in 4% paraformaldehyde for 3 days, defatted for 3 days, and decalcified with 10% EDTA for 7–21 days. Discs were paraffin-embedded, and consecutive 5 μm sections were stained with hematoxylin and eosin (H&E) or Safranin-O (Merck; Darmstadt, Germany) and fast green (Sigma-Aldrich, St Louis, MO). Immunohistochemical (IHC) staining was then performed for thrombin (sc271449, 1:100, Santa Cruz Biotechnology), MCP-1 (#2029, 1:100, Cell Signaling Technology, Danvers, MA, USA), Iba-1 (013-27691, 1:1000, Fujifilm, Tokyo, Japan), iNOS (MAB9502, 1:50, R&D Systems, Minneapolis, MN, USA), Arginase-1 (#93668, 1:100, Cell Signaling Technology), CD86 (NBP2-25208, 1:250, Novus Biologicals, Centennial, CO, USA), CD163 (ab182422, 1:500, Abcam, Cambridge, MA, USA), VEGF (sc152, 1:50, Santa Cruz Biotechnology, Inc.), CD31 (#77699, 1:100, Cell Signaling Technology), or control IgG, using the Liquid DAB + Substrate Chromogen System (Dako, Carpinteria, CA, USA) according to the manufacturer's specifications, with counterstaining using hematoxylin.

Quantitative real-time reverse transcription PCR (qRT–PCR)

Quantitative RT–PCR was performed as previously described [49]. In brief, mIVD tissues (nine discs, ~ 10 μg in total) were collected, and total RNA was extracted using the RNeasy mini kit, with quality check analysis performed using NanoDrop (Thermo Fisher Scientific), followed by treatment with DNase (Qiagen, Venlo, Netherlands), according to the manufacturer's instructions. Complementary DNA was synthesized from 2 μg of

total RNA using a Reverse Transcriptase System (Applied Biosystems, Foster City, CA, USA). Quantitative real-time PCR analysis of the cDNA from each mouse was performed using the StepOnePlus Real-Time PCR System (Applied Biosystems). The thermal cycling conditions were as follows: 95 °C for 20 s followed by 40 cycles of 95 °C for 1 s and 60 °C for 20 s. The primers and probes for murine MCP-1 (Mm 00441242_m1), murine CD86 (Mm00444540_m1), murine CD163 (Mm00474091_m1), VEGF (Mm00437306_m1), and murine hypoxanthine phosphoribosyltransferase (Mm03024075_m1) were purchased from Applied Biosystems. Relative mRNA levels were quantified using the ΔCt method and normalized to those of HPRT [50].

ELISA

mIVDs were cultured in 12-well plates. The conditioned media were collected and prepared by microcentrifugation at 4000×*g* for 5 min, twice. Concentrations of MCP-1 (432704, BioLegend) and VEGF (DY493-05, R&D Systems) in the conditioned media were determined using a Quantikine Colorimetric Sandwich ELISA Kit, according to the manufacturer's specifications. Absorbance was measured using a microplate reader SH-1100R (Lab; Corona Electric Co., Ltd., Ibaraki, Japan).

Murine macrophage preparation

Bone marrow-derived cells were collected from the femurs of 6-week-old C57BL/6 J mice. After removing the soft tissue surrounding the femur, both bone ends were removed. A 23-gauge needle was inserted at one end, and PBS (Life Technologies Japan) was injected to wash out the bone marrow-derived cells. The cells were collected via centrifugation and placed in a 12-well plate. Cells were cultured in a growth medium comprising DMEM (4.5 g/L glucose; Invitrogen) containing 10% fetal calf serum, 100 U/mL penicillin, and 100 μg/mL streptomycin, in a humidified atmosphere at 37 °C with 5% CO_2 for 3 days. Subsequently, thrombin (100 nM) was added, and stimulation was performed for time periods appropriate to each assay. The cells were routinely subjected to mycoplasma testing using MycoAlert® Mycoplasma Detection Kits (Lonza, Basel, Switzerland).

Western blotting

mIVD tissues (nine discs) were collected, and a protein assay was performed for quantitative analysis of the nucleus pulposus and annulus fibrosis (AF), using CelLytic MT cell lysis reagent (Sigma-Aldrich), according to the manufacturer's instructions. Equal amounts of protein from each sample were analyzed, as previously described [51], using immunoblotting with primary antibodies against iNOS (MAB9502, 1:500, R&D Systems), CD86 (NBP2-25208, 1:250, Novus Biologicals), Arginase-1 (#93668, 1:1000, Cell Signaling Technology), CD163 (ab182422, 1:1000, Abcam), and β-actin (A2228, 1:1000, Sigma-Aldrich). β-actin was used for normalization of relative protein levels. After three washes, the membranes were treated with anti-mouse or anti-rabbit secondary antibodies conjugated with horseradish peroxidase (#7076, 1:2000, or #7074, 1:2000, Cell Signaling Technology) for 2 h. Images were captured using ChemiDoc Touch imager (Bio-Rad, Hercules, CA, USA) and quantified using ImageJ (National Institutes of Health, Bethesda, MA, USA).

Statistical analysis

Data are presented as the mean ± standard deviation (SD). Statistical analysis was performed using Statcel-the Useful Addin Forms on Excel-4th ed (OMS Publishing, Tokyo, Japan). Significance was determined using Student's or Welch's *t*-test after an *F*-test was performed for equality of variances, unless otherwise stated. The normality of data was assessed using the Shapiro–Wilk test, except when the raw data did not fit a normal distribution, when the Mann–Whitney *U*-test was used. Differences were considered significant at $p < 0.05$.

Data availability

The datasets used and/or analyzed in the current study are available from the corresponding author upon reasonable request.

Received: 14 August 2024; Accepted: 3 September 2025
Published online: 06 October 2025

References

1. Hestbaek, L., Leboeuf-Yde, C. & Kyvik, K. O. Are lifestyle-factors in adolescence predictors for adult low back pain? A cross-sectional and prospective study of young twins. *BMC Musculoskelet Disord.* **7**, 27 (2006).
2. GBD 2021 Low Back Pain Collaborators. Global, regional, and national burden of low back pain, 1990–2020, its attributable risk factors, and projections to 2050: A systematic analysis of the Global Burden of Disease Study 2021. *Lancet Rheumatol.* **5**, e316–e329 (2023).
3. Hartvigsen, J. et al. What low back pain is and why we need to pay attention. *Lancet* **391**, 2356–2367 (2018).
4. Chen, S. et al. Global, regional and national burden of low back pain 1990–2019: A systematic analysis of the Global Burden of Disease study 2019. *J. Orthop. Translat.* **32**, 49–58 (2022).
5. Wu, A. et al. Global low back pain prevalence and years lived with disability from 1990 to 2017: Estimates from the Global Burden of Disease Study 2017. *Ann. Transl. Med.* **8**, 299 (2020).
6. Hoy, D. et al. The global burden of low back pain: Estimates from the Global Burden of Disease 2010 study. *Ann. Rheum Dis.* **73**, 968–974 (2014).
7. Driscoll, T. et al. The global burden of occupationally related low back pain: Estimates from the Global Burden of Disease 2010 study. *Ann. Rheum Dis.* **73**, 975–981 (2014).
8. Maher, C., Underwood, M. & Buchbinder, R. Non-specific low back pain. *Lancet* **389**, 736–747 (2017).
9. Hoy, D., Brooks, P., Blyth, F. & Buchbinder, R. The epidemiology of low back pain. *Best Pract. Res. Clin. Rheumatol.* **24**, 769–781 (2010).
10. Iwasaki, T. et al. Expression of glial-cell-line-derived neurotrophic factor family ligands in human intervertebral discs. *Int. J. Mol. Sci.* **24** (2023).

11. Yamamoto, T. et al. Efficacy of hyaluronic acid on intervertebral disc inflammation: An in vitro study using notochordal cell lines and human disc cells. *J. Orthop. Res.* **39**, 2197–2208 (2021).
12. Suyama, K. et al. Effects of interleukin-17A in nucleus pulposus cells and its small-molecule inhibitors for intervertebral disc disease. *J. Cell. Mol. Med.* **22**, 5539–5551 (2018).
13. Miyagi, M. et al. ISSLS Prize winner: Increased innervation and sensory nervous system plasticity in a mouse model of low back pain due to intervertebral disc degeneration. *Spine (Phila Pa 1976)* **39**, 1345–1354 (2014).
14. Ohtori, S. et al. Results of surgery for discogenic low back pain: A randomized study using discography versus discoblock for diagnosis. *Spine (Phila Pa 1976)* **34**, 1345–1348 (2009).
15. van Uden, S., Silva-Correia, J., Oliveira, J. M. & Reis, R. L. Current strategies for treatment of intervertebral disc degeneration: Substitution and regeneration possibilities. *Biomater. Res.* **21**, 22 (2017).
16. Huang, Y. C., Urban, J. P. & Luk, K. D. Intervertebral disc regeneration: Do nutrients lead the way?. *Nat. Rev. Rheumatol.* **10**, 561–566 (2014).
17. Haro, H., Kato, T., Komori, H., Osada, M. & Shinomiya, K. Vascular endothelial growth factor (VEGF)-induced angiogenesis in herniated disc resorption. *J. Orthop. Res.* **20**, 409–415 (2002).
18. Komori, H. et al. Contrast-enhanced magnetic resonance imaging in conservative management of lumbar disc herniation. *Spine (Phila Pa 1976)* **23**, 67–73 (1998).
19. Mochida, K. et al. Regression of cervical disc herniation observed on magnetic resonance images. *Spine (Phila Pa 1976)* **23**, 990–995 (1998) (**discussion 996-997**).
20. Ohba, T. et al. TNF-alpha-induced NF-kappaB signaling reverses age-related declines in VEGF induction and angiogenic activity in intervertebral disc tissues. *J. Orthop. Res.* **27**, 229–235 (2009).
21. Sato, N. et al. Thrombin induced by the extrinsic pathway and PAR-1 regulated inflammation at the site of fracture repair. *Bone* **83**, 23–34 (2016).
22. Ichikawa, J. et al. Thrombin induces osteosarcoma growth, a function inhibited by low molecular weight heparin in vitro and in vivo: Procoagulant nature of osteosarcoma. *Cancer* **118**, 2494–2506 (2012).
23. Takayama, Y., Ando, T., Ichikawa, J. & Haro, H. Effect of thrombin-induced MCP-1 and MMP-3 production via PAR1 expression in murine intervertebral discs. *Sci. Rep.* **8**, 11320 (2018).
24. Huang, B. R. et al. EGFR is a pivotal regulator of thrombin-mediated inflammation in primary human nucleus pulposus culture. *Sci. Rep.* **7**, 8578 (2017).
25. Wang, J. et al. The role of macrophage polarization and associated mechanisms in regulating the anti-inflammatory action of acupuncture: a literature review and perspectives. *Chin. Med.* **16**, 56 (2021).
26. Gordon, S. Alternative activation of macrophages. *Nat. Rev. Immunol.* **3**, 23–35 (2003).
27. Yunna, C., Mengru, H., Lei, W. & Weidong, C. Macrophage M1/M2 polarization. *Eur. J. Pharmacol.* **877**, 173090 (2020).
28. Yamamoto, Y. et al. Distribution and polarization of hematogenous macrophages associated with the progression of intervertebral disc degeneration. *Spine (Phila Pa 1976)* **47**, E149–E158 (2022).
29. Yamagishi, A., Nakajima, H., Kokubo, Y., Yamamoto, Y. & Matsumine, A. Polarization of infiltrating macrophages in the outer annulus fibrosus layer associated with the process of intervertebral disc degeneration and neural ingrowth in the human cervical spine. *Spine J.* **22**, 877–886 (2022).
30. Dou, Y. et al. Role of macrophage in intervertebral disc degeneration. *Bone Res.* **13**, 15 (2025).
31. Ohnishi, T. et al. In vivo mouse intervertebral disc degeneration model based on a new histological classification. *PLoS ONE* **11**, e0160486 (2016).
32. Fujita, K. et al. Age-related expression of MCP-1 and MMP-3 in mouse intervertebral disc in relation to TWEAK and TNF-alpha stimulation. *J. Orthop. Res.* **30**, 599–605 (2012).
33. Martinez, F. O. & Gordon, S. The M1 and M2 paradigm of macrophage activation: Time for reassessment. *F1000Prime Rep.* **6**, 13 (2014).
34. Heideveld, E. et al. Glucocorticoids induce differentiation of monocytes towards macrophages that share functional and phenotypical aspects with erythroblastic island macrophages. *Haematologica* **103**, 395–405 (2018).
35. Van Dyken, S. J. & Locksley, R. M. Interleukin-4- and interleukin-13-mediated alternatively activated macrophages: Roles in homeostasis and disease. *Annu. Rev. Immunol.* **31**, 317–343 (2013).
36. Lopez-Zambrano, M., Rodriguez-Montesinos, J., Crespo-Avilan, G. E., Munoz-Vega, M. & Preissner, K. T. Thrombin promotes macrophage polarization into M1-like phenotype to induce inflammatory responses. *Thromb. Haemost.* **120**, 658–670 (2020).
37. Tomasello, S. D., Angiolillo, D. J. & Goto, S. Inhibiting PAR-1 in the prevention and treatment of atherothrombotic events. *Expert. Opin. Investig. Drugs* **19**, 1557–1567 (2010).
38. Angiolillo, D. J., Capodanno, D. & Goto, S. Platelet thrombin receptor antagonism and atherothrombosis. *Eur. Heart J.* **31**, 17–28 (2010).
39. Coughlin, S. R. Thrombin signalling and protease-activated receptors. *Nature* **407**, 258–264 (2000).
40. Fala, L. Zontivity (Vorapaxar), first-in-class PAR-1 antagonist, receives FDA approval for risk reduction of heart attack, stroke, and cardiovascular death. *Am. Health Drug Benefits* **8**, 148–151 (2015).
41. Chaudhary, R. et al. Improving outcomes in cardiovascular diseases: a review on Vorapaxar. *Cardiol. Rev.* **30**, 241–246 (2022).
42. Teraguchi, M. et al. Prevalence and distribution of intervertebral disc degeneration over the entire spine in a population-based cohort: The Wakayama Spine Study. *Osteoarthr. Cartil.* **22**, 104–110 (2014).
43. Haro, H. et al. Matrix metalloproteinase-3-dependent generation of a macrophage chemoattractant in a model of herniated disc resorption. *J. Clin. Invest.* **105**, 133–141 (2000).
44. Haro, H. et al. Matrix metalloproteinase-7-dependent release of tumor necrosis factor-alpha in a model of herniated disc resorption. *J. Clin. Invest.* **105**, 143–150 (2000).
45. Romaniyanto, F. et al. Effectivity of puncture method for intervertebral disc degeneration animal models: Review article. *Ann. Med. Surg.* **85**, 3501–3505 (2023).
46. Ohta, R. et al. Heme oxygenase-1 modulates degeneration of the intervertebral disc after puncture in Bach 1 deficient mice. *Eur. Spine J.* **21**, 1748–1757 (2012).
47. Percie du Sert, N. et al. The ARRIVE guidelines 2.0: Updated guidelines for reporting animal research. *J. Physiol.* **598**, 3793–3801 (2020).
48. Fujimaki, T. et al. Exogenous parathyroid hormone attenuates ovariectomy-induced skeletal muscle weakness in vivo. *Bone* **151**, 116029 (2021).
49. Ichikawa, J. et al. Role of platelet C-type lectin-like receptor 2 in promoting lung metastasis in osteosarcoma. *J. Bone Min. Res.* **35**, 1738–1750 (2020).
50. Livak, K. J. & Schmittgen, T. D. Analysis of relative gene expression data using real-time quantitative PCR and the 2(-Delta Delta C(T)) Method. *Methods* **25**, 402–408 (2001).
51. Ando, T. et al. Gemcitabine and rapamycin exhibit additive effect against osteosarcoma by targeting autophagy and apoptosis. *Cancers* **12** (2020).

Acknowledgements

The authors thank Tadashi Iwato, Chizuru Chino, and Mika Ubagai for their technical assistance, and Kahori

Sano and Azusa Sakamoto for secretarial assistance. We would like to thank Editage (www.editage.com) for English language editing. This research was funded by JSPS KAKENHI (19K09594, and 23K08584).

Author contributions

Conceptualization: R.T., H.H., and T.A. Methodology: R.T., Y.T., and T.A. Data Analysis: R.T. and Y.T. Data Curation: R.T., T.A., T.F., Y.T., and T.O. Writing—Original Draft: R.T. and T.A. Writing—Review and Editing: R.T., T.A., and H.H. All authors take responsibility for the integrity of the data analysis, have reviewed the results, and have approved the final version of the manuscript.

Declarations

Competing interests

The authors declare no competing interests.

Additional information

Supplementary Information The online version contains supplementary material available at https://doi.org/10.1038/s41598-025-18684-6.

Correspondence and requests for materials should be addressed to T.A.

Reprints and permissions information is available at www.nature.com/reprints.

Publisher's note Springer Nature remains neutral with regard to jurisdictional claims in published maps and institutional affiliations.